



**Acoustics'08
Paris**
June 29-July 4, 2008

www.acoustics08-paris.org

Fluid-structure interaction and computational aeroacoustics of the flow past a thin flexible structure

Frank Schäfer^a, Thomas Uffinger^a, Stefan Becker^a, Jens Grabinger^b and
Manfred Kaltenbacher^b

^aUniversity Erlangen-Nuremberg, Institute of Fluid Mechanics, Cauerstr. 4, 91058 Erlangen,
Germany

^bUniv. Erlangen-Nuremberg, Dept. of Sensor Technology, Paul-Gordan-Str. 3/5, 91052
Erlangen, Germany
frank.schaefer@lstm.uni-erlangen.de

In the present work, the acoustic field resulting from the interaction of a thin flexible structure with a turbulent flow field is investigated by means of numerical simulation. Two different model configurations are considered: one is the flow over a flexible plate, in the second case the flexible plate is located in the wake of a square cylinder. The simulation is based on a partitioned approach employing two different simulation codes: a finite-volume flow solver of second order accuracy in space and time and a finite-element structural mechanics and acoustics solver. A code coupling interface is used for the exchange of data between the different discretizations. The numerical methodology allows for a decomposition of the acoustic field into one part generated by the structural vibrations and another part which is due to stream noise. Comparisons to experimental data available at our institute are provided.

1 Introduction

In many technical applications the flow of a fluid past a flexible plate-like structure leads to structural vibrations and thereby to the generation of vibrational sound. Coverings and panelings of cars and airplanes are important examples for this kind of fluid-structure-acoustic interaction. Usually, the sound generated by the flow induced vibrations is considered as noise so that its reduction is a topic of major interest.

In the present work, the acoustic field resulting from the interaction of a thin flexible structure with a turbulent flow is investigated by means of numerical simulation. A test case was developed which represents a simplified model of a car underbody. A description of the test case is given in section 2. The simulation is based on a partitioned approach employing a finite-volume flow solver and a finite-element structural mechanics and acoustics solver. A code coupling interface is used for the exchange of data between the finite-volume and the finite-element discretization. An important feature of the computational scheme is that it allows for a separate prediction of flow induced and vibrational sound. Further details about the numerical methods are given in section 3. Finally, the results of the study concerning the vibration of the flexible plate and the generated sound are presented in section 4. Comparisons to experimental data available at our institute are also provided.

2 Test Case

The basic setup of the test case considered in the present work consists of a flexible plate-like structure which is part of an otherwise rigid wall. In order to study the influence of geometric flow disturbances on the resulting acoustic field, two different configurations have been investigated: one case with a square cylinder obstacle in front of the flexible plate as shown in figure 1(a), and a second case without obstacle (see figure 1(b)). In the remainder of the paper, the two configurations are referred to as case A and B, respectively.

A flow of air at ambient conditions is considered. The free-stream velocity U_∞ is set to 20 m/s. The plate is made of stainless steel with a thickness of 40 μm (density $\rho_s = 7850 \text{ kg/m}^3$, modulus of elasticity $E = 2 \cdot 10^{11} \text{ kg/ms}^2$, Poisson number $\nu = 0.3$, pre-stressing in streamwise direction $7 \cdot 10^6 \text{ N/m}^2$). In case A, the edge length of the square cylinder is $D = 0.02 \text{ m}$. The streamwise extension of the flexible plate amounts to $7.5D$ in both configurations. Because of the pre-stressing the plate is clamped over a length of $0.5D$ at the upstream and the downstream edge, respectively.

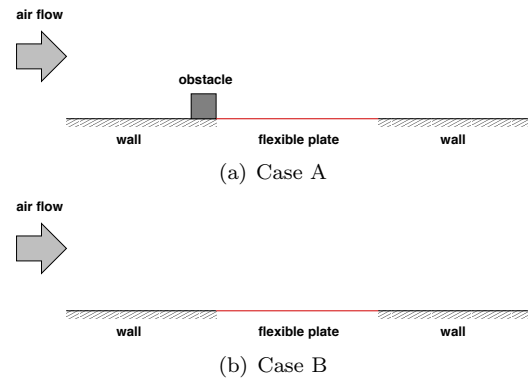


Figure 1: Setup of the test case

3 Numerical Method

A partitioned computation scheme is used for the simulation of the fluid-structure-acoustic interaction of the present test case. Two different simulation codes are employed. The numerical flow computation is carried out with FASTEST-3D [1], a finite-volume CFD solver developed at the Institute of Fluid Mechanics, University of Erlangen-Nuremberg. For the structural mechanics and the acoustics computations the finite-element multiphysics solver CFS++ [2] is applied, which has been developed at the Department of Sensor Technology, University of Erlangen-Nuremberg.

In the present computation scheme, the effect of the acoustics on the structure and the fluid is neglected since the expected acoustic pressure fluctuations are much smaller than the overall fluid pressure. Therefore, the fluid-structure-acoustic interaction can be split into three parts which are treated independently: fluid-structure interaction, fluid-acoustic coupling and structure-acoustic coupling. A detailed description of the resulting computation scheme can be found in Schäfer et al. [3, 4]. For fluid-structure interaction an implicit coupling between FASTEST-3D and CFS++ is applied. The exchange of data between the finite-volume and the finite-element discretization is realized by MpCCI [5]. The acoustic computations are performed with CFS++ using a finite-element discretization of the wave equation which describes the propagation of sound to the far field. Structure-acoustic coupling is done in CFS++ by applying appropriate boundary conditions to the wave equation [4]. The computation of flow induced noise (fluid-acoustic coupling) is based on our finite-element formulation of Lighthill's analogy [6].

The flow simulation is carried out by solving the incompressible Navier-Stokes equations with discretiza-

tions of second order accuracy in both space and time. The considered flow domain for configuration A is depicted in figure 2(a). Basically, the same setup is used for configuration B, but without obstacle. The computations are performed as large-eddy simulations (LES) with the Smagorinsky model and an implicit time discretization scheme. Since all boundary layers have to be resolved properly, block-structured meshes with up to 8 million control volumes are used for the spatial discretization of the flow domain.

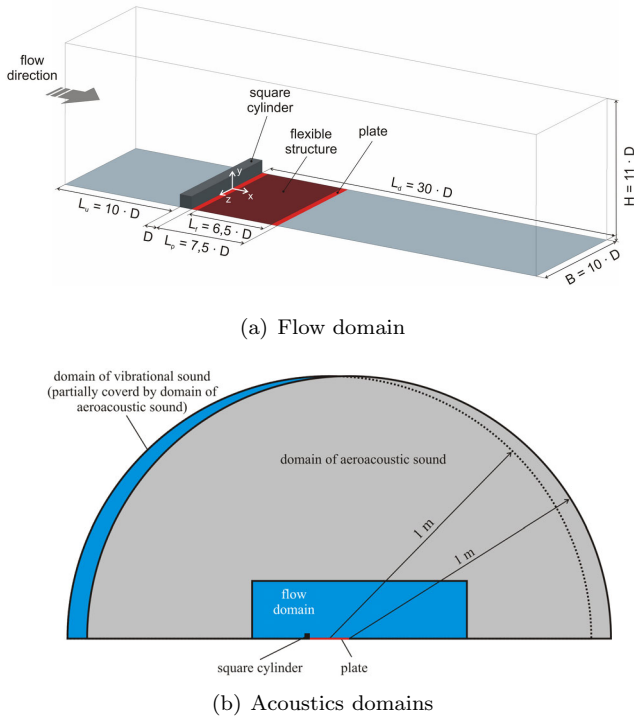


Figure 2: Computational domains for case A

For the structural mechanics computation the flexible plate is discretized using 13 000 hexahedral elements. Linear basis functions with an incompatible mode approach to account for shear locking effects are applied together with an implicit second order time discretization scheme of the Newmark type [7]. In accordance with the specification of the test case, the flexible plate is pre-stressed in the streamwise direction.

The computational domains for acoustics are larger than the flow domain since we are interested in the radiation of noise to the far field. A schematic is shown in figure 2(b). Up to 420 000 linear elements are used for the spatial discretization of the acoustic domains. Absorbing boundary conditions are applied at the top boundary in order to guarantee for free radiation conditions. For the simulation of vibrational sound non-conforming finite elements are used at the interface between structural mechanics and acoustics.

4 Results

4.1 Flexible plate with square cylinder

A comparison of the averaged velocity field obtained by simulation and laser-Doppler anemometry (LDA) measurements, respectively, is provided in figure 3. The

most prominent flow structure is a large region of recirculation which is located behind the square cylinder. The overall agreement between simulation and experiment is very good. The computed and the measured length of the recirculation region are almost the same. There is only a minor difference in recirculation length which is measured somewhat shorter in the experiments.

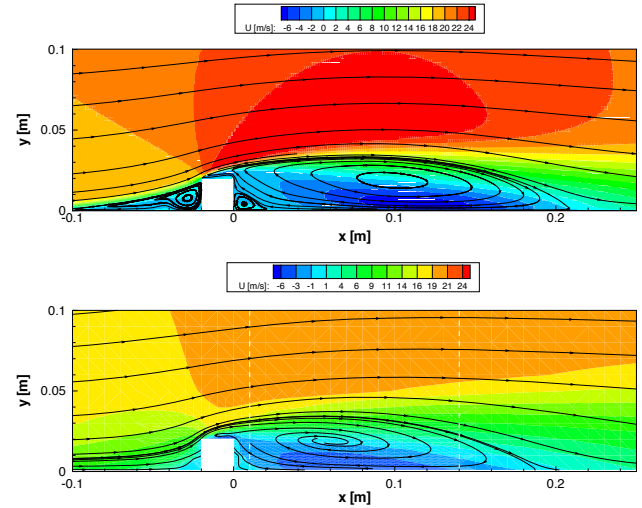
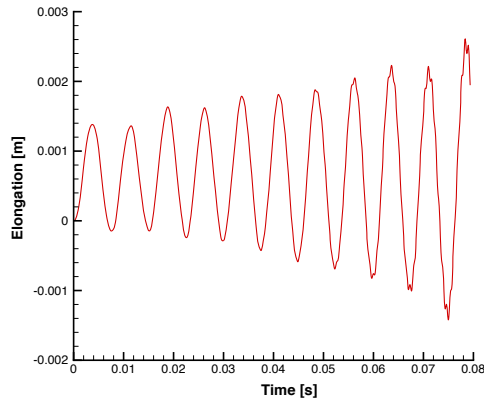


Figure 3: Average velocity in main flow direction for case A: simulation (top) and experiment (bottom)

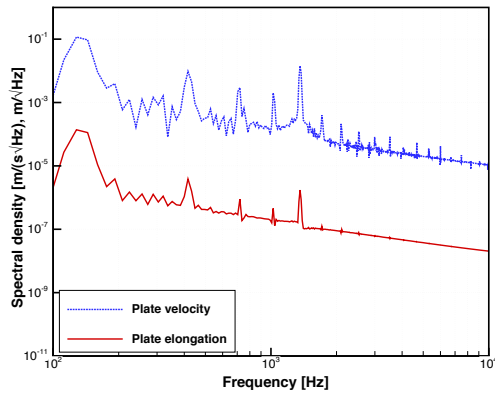
The computed displacements of the flexible plate due to fluid-structure interaction are shown in figure 4. Figure 4(a) depicts the temporal evolution of the elongation of a point in the center of the flexible plate. Before $t = 0$ the flow is computed without fluid-structure interaction in order to obtain a fully developed turbulent flow over the square cylinder. At $t = 0$ the plate is made flexible and fluid-structure interaction is initiated. As can be seen from the diagram, the plate starts oscillating with an average displacement in the upwards direction which is due to the local pressure minimum located in the recirculation region behind the square cylinder. Below the plate ambient pressure is assumed. The frequency of the oscillation is about 140 Hz, which is in very good agreement with the first eigenfrequency of the plate at 142 Hz. The increase in amplitude which can be observed over time is possibly related to the geometrically linear model used in the structural mechanics computations [8].

Frequency spectra of the plate elongation and the plate velocity are shown in figure 4(b). Besides the first eigenfrequency, also higher oscillation modes are excited which are very close to the odd eigenfrequencies of the flexible plate. All observed modes are more or less homogeneous in the spanwise direction. The amplitudes of the higher-frequency modes are small compared to the first eigenmode so that they are of minor importance.

The flow induced sound and the vibrational sound have been calculated separately. The resulting flow induced sound based on the Lighthill analogy is shown in figure 5. The frequency spectra of the sound pressure level (SPL) in figure 5(a) exhibit a broadband character with an elevation between 100 and 200 Hz. In the phase of the simulation before starting the fluid-structure interaction this elevation cannot be found. It seems that there is a slight influence of the plate vibra-



(a) Elongation of a point in the center of the plate



(b) Frequency spectra of the elongation and the velocity of a point in the center of the plate

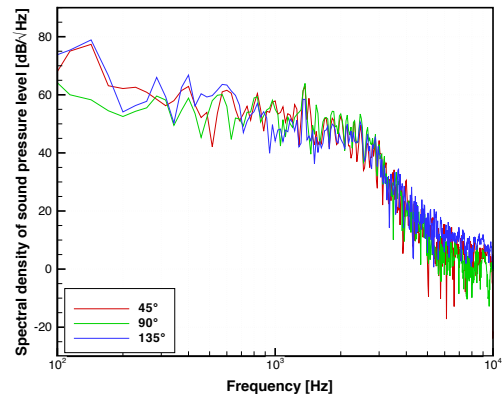
Figure 4: Displacement of the flexible plate (case A)

tion on the flow induced sound. The directivity pattern in figure 5(b) is comparable to a dipole with a neutral axis varying between 60 and 90 degree, where angle zero corresponds to the main flow direction. However, at some frequencies significant deviations from the dipole characteristics can be observed. Again, the picture is different in the phase of the simulation before starting the fluid-structure interaction, where a dipole directivity with a neutral axis at 60 degree is constantly found over a wide range of frequencies.

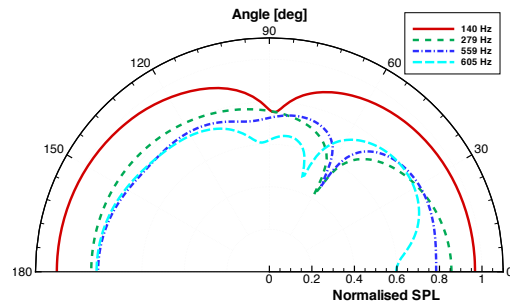
Frequency spectra of the computed vibrational sound pressure level are plotted in figure 6. A prominent peak can be found next to the first eigenfrequency of the plate, together with several higher-frequency peaks corresponding to the higher oscillation modes of the plate. This is in very good accordance with the spectra of the plate oscillation presented in figure 4(b).

4.2 Flexible plate without obstacle

The computed displacements of the flexible plate without square cylinder are shown in figure 7. Qualitatively, the results are very similar to those obtained for case A (compare figure 4). However, significant quantitative differences can be found. Most importantly, without obstacle the amplitudes of the oscillation are by a factor of about 10 smaller than with square cylinder. The same has been observed for the computed fluid load on the plate. This indicates that the excitation of the plate by



(a) Frequency spectra at 45, 90 and 135 degree



(b) Directivity pattern at different frequencies

Figure 5: Computed flow induced sound in a distance of 1 m from the downstream edge of the plate (case A)

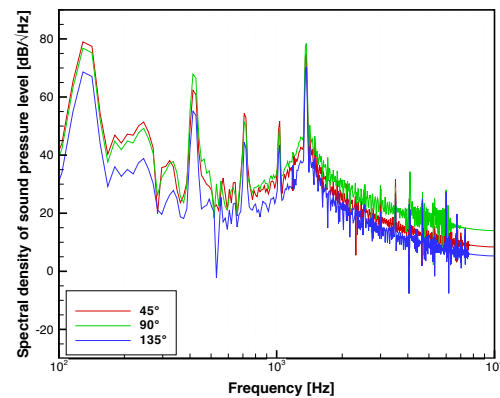
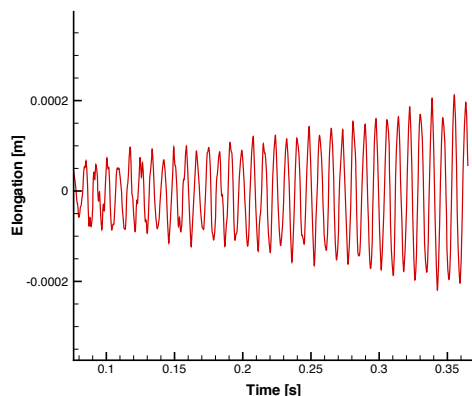


Figure 6: Computed vibrational sound in a distance of 1 m from the center of the plate (case A)

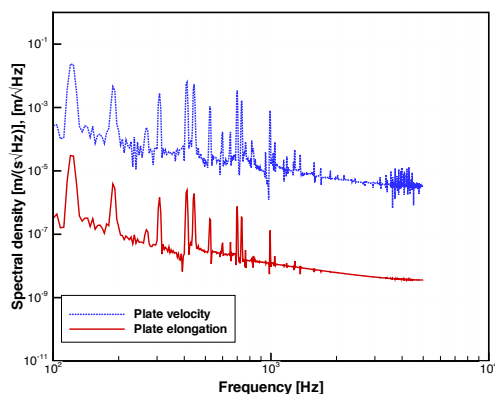
the turbulent boundary layer in case B is much weaker than by the flow in the wake of the square cylinder in case A.

Frequency spectra of the plate elongation and the plate velocity are plotted in figure 7(b). Compared to case A, the frequency of the most dominant mode is shifted towards 120 Hz which is significantly less than the first eigenfrequency of the plate at 142 Hz. The same applies to the observed higher frequency modes which do not coincide with the odd eigenfrequencies of the plate, but can be related to other, partly non-homogeneous eigenmodes.

The computed flow induced sound is displayed in figure 8. A broadband frequency spectrum can be ob-



(a) Elongation of a point in the center of the plate



(b) Frequency spectra of the elongation and the velocity of a point in the center of the plate

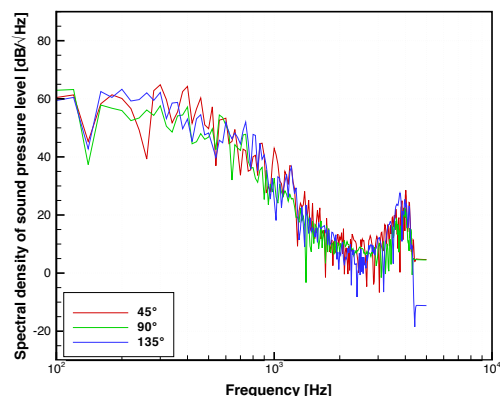
Figure 7: Displacement of the flexible plate (case B)

served with no significant elevation in the vicinity of the plate's major oscillation frequency. Flow induced sound and plate vibration seem to be fully decoupled, while in case A a slight influence of the plate vibration was found. This might be attributed to the smaller vibration amplitude in case B, which certainly leads to a smaller influence of the vibration on the flow field. Apart from the elevation between 100 and 200 Hz in case A, below 400 Hz the computed sound pressure level is of the same order of magnitude in both cases A and B. Above 400 Hz, a more rapid decrease is seen for the case without obstacle.

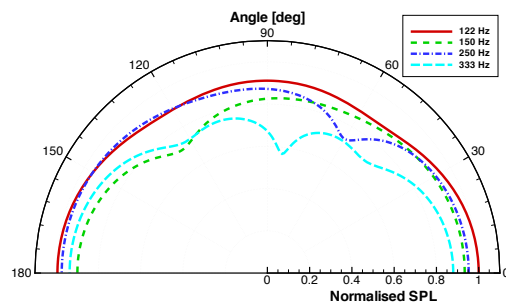
The computed vibrational sound is plotted in figure 9. It is found that the amplitudes of the most prominent peaks are significantly lower than in case A. This is in accordance with expectation since in case B the vibration amplitude of the plate is by approximately one order of magnitude smaller than in case A, while the vibration frequency is similar. This leads to a smaller plate velocity and thereby to a reduced acoustic particle velocity and sound pressure.

4.3 Comparison to experimental data

Frequency spectra of the measured sound pressure level are plotted in figure 10. Spectra obtained for the empty test section, for the flexible plate without square cylinder (case B) and for the flexible plate with square cylinder (case A) are provided. In comparison to the empty



(a) Frequency spectra at 45, 90 and 135 degree



(b) Directivity pattern at different frequencies

Figure 8: Computed flow induced sound in a distance of 1 m from the downstream edge of the plate (case B)

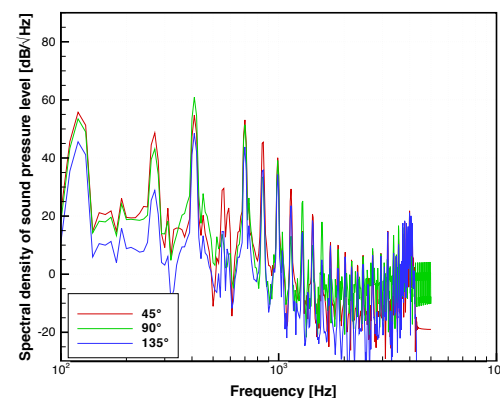


Figure 9: Computed vibrational sound in a distance of 1 m from the center of the plate (case B)

test section, the case of the flexible plate without obstacle shows several peaks in the range between 100 and 200 Hz, which corresponds approximately to the first eigenfrequency of the plate. For higher frequencies, there is only a small difference to the reference case with the empty test section. The presence of the square cylinder obstacle leads to a significant increase in sound pressure level in the range between 100 and 200 Hz, with a prominent peak at about 115 Hz. Additionally, at higher frequencies a large increase in broadband noise is observed.

Comparing the frequency spectra of the computed sound pressure level with the experimental findings in figure 10, despite of quantitative differences it can be

noticed that the overall tendency in the experiment is very well reflected by the simulation. In both experiment and simulation the flow disturbance caused by the square cylinder leads to a significant increase in sound pressure level compared to the case without obstacle. In this respect, the tonal component observed between 100 and 200 Hz in the measurements corresponds well to the computed vibrational sound due to the first eigenmode of the plate. However, modes beyond the first eigenfrequency which are found in the simulations cannot be clearly observed in the experiments. This might indicate that the damping of the current computational structure model is somewhat low at high frequencies.

In the square cylinder case, the computed flow induced noise was found to be more intense at high frequencies than in the case without square cylinder. Qualitatively, this is in good accordance with the experiments where broadband noise is observed in the high frequency range in case A while it is not present in case B. Hence, the numerical results indicate that this broadband noise is not due to the plate vibration but due to the turbulent flow past the square cylinder.

The most important difference between experiment and simulation is that the computed sound pressure levels are significantly higher than the measured values. However, as far as the vibrational sound is concerned, this is only true for the peak values. Between the peaks the computed and the measured levels are of the same order of magnitude. The high peak values of the computed sound pressure can be attributed to the increasing amplitude of the simulated plate oscillation shown in figures 4(a) and 7(a). Increasing amplitude at the same frequency leads to increasing plate velocity and thereby to higher sound pressure values. We expect that this will change if a geometrically non-linear model is used in the structural mechanics computation.

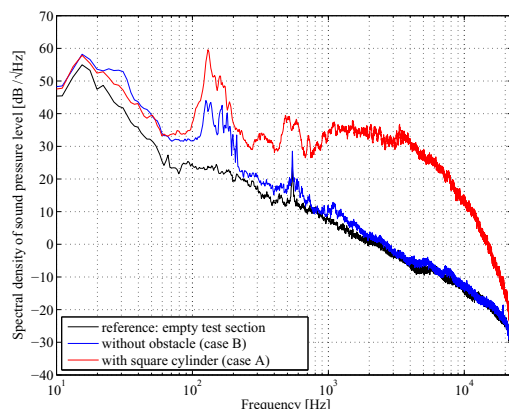


Figure 10: Measured sound pressure level

5 Conclusion

Numerical investigations of the noise produced by the flow over a thin flexible plate were presented. Two different configurations were considered: one case with a square cylinder obstacle located in front of the flexible plate, and one case without obstacle. The applied computational scheme allowed for a separate determination

of flow induced and vibrational sound, which is generally very difficult to achieve experimentally.

The overall tendency of the computed sound pressure levels was in good accordance with available experimental data. However, over a wide range of frequencies the predicted values were too high. To resolve this problem, in the structural mechanics computation a non-linear model should be used in future work.

Acknowledgements

Financial Support by the Bavarian Research Foundation is gratefully acknowledged.

References

- [1] Durst, F. & Schäfer, M.: *A Parallel Block-Structured Multigrid Method for the Prediction of Incompressible Flows*. International Journal of Numerical Methods Fluids, vol. 22, pp. 549–565, 1996.
- [2] Kaltenbacher, M., Hauck, A., Triebenbacher, S., Link, G. & Bahr, L.: *CFS++: Coupled Field Simulation*. 2007.
- [3] Schäfer, F., Ali, I., Becker, S., Kaltenbacher, M., Escobar, M. & Link, G.: *Computational Aeroacoustics using MpCCI as Coupling Interface between Fluid Mechanics, Structural Mechanics and Acoustics*. In *Proceedings of the 7th MpCCI User Forum*, pp. 98–111, February 21–22, 2006.
- [4] Schäfer, F., Kniesburges, S., Uffinger, T., Becker, S., Grabinger, J., Link, G. & Kaltenbacher, M.: *Numerical Simulation of Fluid-Structure- and Fluid-Structure-Acoustic Interaction based on a Partitioned Coupling Scheme*. In *High Performance Computing in Science and Engineering, Munich 2007*, Springer, 2008 (to appear).
- [5] Ahrem, R., Hackenberg, M. G., Redler, R. & Roggenbunck, J.: *MpCCI Mesh Based Parallel Code Coupling Interface*. Institute of Algorithms and Scientific Computing (SCAI), GMD, <http://www.mpcci.org/>, 2003.
- [6] Kaltenbacher, M., Escobar, M., Becker, S. & Ali, I.: *Computational Aeroacoustics based on Lighthill's Analogy*. In *Computational Acoustics of Noise Propagation in Fluids*, pp. 115–142, Springer, 2008.
- [7] Kaltenbacher, M.: *Numerical Simulation of Mechatronic Sensors and Actuators*. Springer, 2nd edition, 2007.
- [8] Rifai, S. M., Johan, Z., Wang, W.-P., Grisval, J.-P., Hughes, T. J. R. & Ferencz, R. M.: *Multiphysics simulation of flow-induced vibrations and aeroelasticity on parallel computing platforms*. Computer Methods in Applied Mechanics and Engineering, vol. 174, pp. 393–417, 1998.